Aust. J. Phys., 1984, **37**, 657–65

An Improved Technique for Examining Bragg Reflections in $\Delta\omega, \Delta 2\theta^{(s)}$ Space

A. McL. Mathieson and A. W. Stevenson

Division of Chemical Physics, CSIRO,
P.O. Box 160, Clayton, Vic. 3168.

Abstract

With a standard X-ray tube line source set at right angles to the diffraction plane of a diffractometer and with the usual tube take-off angle, one can obtain, without loss of peak intensity in the Bragg peak, a source which is effectively very small ($\approx 50\ \mu$m) in relation to the diffraction plane. The measured two-dimensional distribution $I(\Delta\omega, \Delta 2\theta^{(s)})$ of a Bragg reflection from a small single crystal then has effectively only two principal components, namely, the mosaic spread of the specimen crystal and the wavelength distribution of the source. This can lead to a relatively direct estimation of the distributions of the two components, that of the mosaic spread being of particular significance for the investigation of the associated factors of reflectivity and extinction.

1. Introduction

The intensity distribution $I(\Delta\omega, \Delta 2\theta^{(s)})$ (for terminology, see Mathieson 1983, 1984*a*) of a Bragg reflection from a small single crystal is a function of several components, each identifiable by its characteristic slope in $\Delta\omega, \Delta 2\theta^{(s)}$ space (Mathieson 1982). In a recent study (Mathieson 1984*b*), the influence of three components which usually make a significant contribution to the two-dimensional distribution, namely the specimen crystal mosaic spread μ, the source emissivity distribution σ (i.e. size) and the wavelength distribution of the source λ, was examined in relation to the derivation of accurate structure factors. In that study, the particular significance of μ was noted because of its identification with the reflectivity distribution of the individual Bragg reflection and hence with the variation of extinction within the one reflection. Because of this relationship, an accurate estimate of the mosaic spread is seen as valuable for the further study of the link between the 'level of interaction' (reflectivity) (Mathieson 1979) and the level of extinction. Under the usual experimental conditions, the number of significant components in the $I(\Delta\omega, \Delta 2\theta)$ distribution is greater than the number of dimensions of the distribution, $\Delta\omega$ and $\Delta 2\theta$, so that estimation of the individual component distributions from the intensity distribution is not necessarily a straightforward process.

It would clearly be advantageous to reduce the size (range) of one or other of the two components not dependent on the specimen, namely the source size and the wavelength distribution, so that there would be only two major components in $\Delta\omega, \Delta 2\theta$ space. A practicable method of achieving this with respect to the source size, without significant loss of peak signal, has been found using a standard X-ray tube.

2. Procedure

For diffractometry with small single crystals, the usual X-ray tube line source is normally disposed so that, with a take-off angle of approximately 1 in 10, the effective source as viewed from the specimen crystal is approximately equi-dimensional, of

0004-9506/84/060657$02.00

dimension between (say) 0·4 mm (semi-microfocus tube) and 1·0 mm (normal focus tube). Fig. 1 illustrates a conventional arrangement where the main length of the X-ray tube is parallel to the diffraction plane, and indicates diagrammatically the three-dimensional distribution $I(\Delta\omega, \Delta 2\theta, p)$ in reciprocal space for a single Bragg reflection in relation to the diffraction plane (see Mathieson 1983), where $\Delta\omega$ and $\Delta 2\theta$ are in the diffraction plane and p is perpendicular to it. Along p, the distribution is essentially monotonic due to (i) the vertical dimension v of the source (see Fig. 1) and (ii) the relaxation of the Bragg condition. Then, with an aperture in front of the (scintillation) detector, which is narrow in the diffraction plane ($\sim$0·1 mm or 0·02°) but extended perpendicular to it, the monotonic signal along p is integrated and one obtains, in practice, the projected two-dimensional distribution $I(\Delta\omega, \Delta 2\theta)$. In this distribution, the horizontal dimension of the effective source h determines the size of the source component σ.

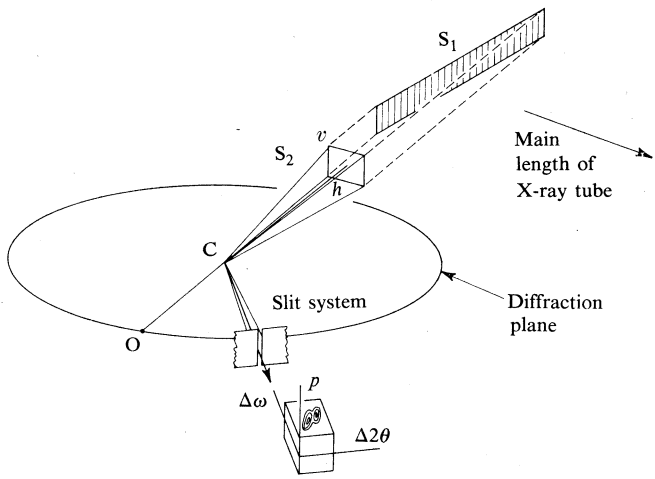

Fig. 1. Conventional experimental arrangement with the main length of the X-ray source S_1 in the plane of diffraction, and where S_2, of width h and height v corresponds to the effective source as seen by the specimen crystal C. The aperture system in front of the (scintillation) detector is narrow in the diffraction plane ($\approx$0·1 mm) and elongated perpendicular to it. The intensity distribution $I(\Delta\omega, \Delta 2\theta, p)$ of a Bragg reflection, with local reference axes $\Delta\omega$, $\Delta 2\theta$ and p, is indicated in relation to the diffraction plane (see Mathieson 1983).

Fig. 2*a* shows a typical distribution $I(\Delta\omega, \Delta 2\theta^{(0)})$ with the type of set-up shown in Fig. 1, in this case for the $\bar{1}\bar{1}2$ reflection of a small crystal (average dimension $\approx$0·06 mm) of tetragonal $CuInSe_2$. The σ component is readily identifiable since it lies at a slope of 45° to the $\Delta 2\theta$ axis and may be more readily recognized in the $s = 1$, ω/θ scan mode (Fig. 2*b*) where σ is at 90° to the $\Delta 2\theta$ axis (see Mathieson 1982). Its dimension in this case, 0·14° in $\Delta\omega$,* corresponds to that of a source of

* In Mathieson (1982), the size of the source was given as $\approx$0·06° which was related to the width at half the peak intensity. For consistency with the later study (Mathieson 1984*a*), where the size of the source was determined at $\approx$10% of the peak intensity, the equivalent value in Mathieson (1982) should be $\approx$0·13–0·14°.

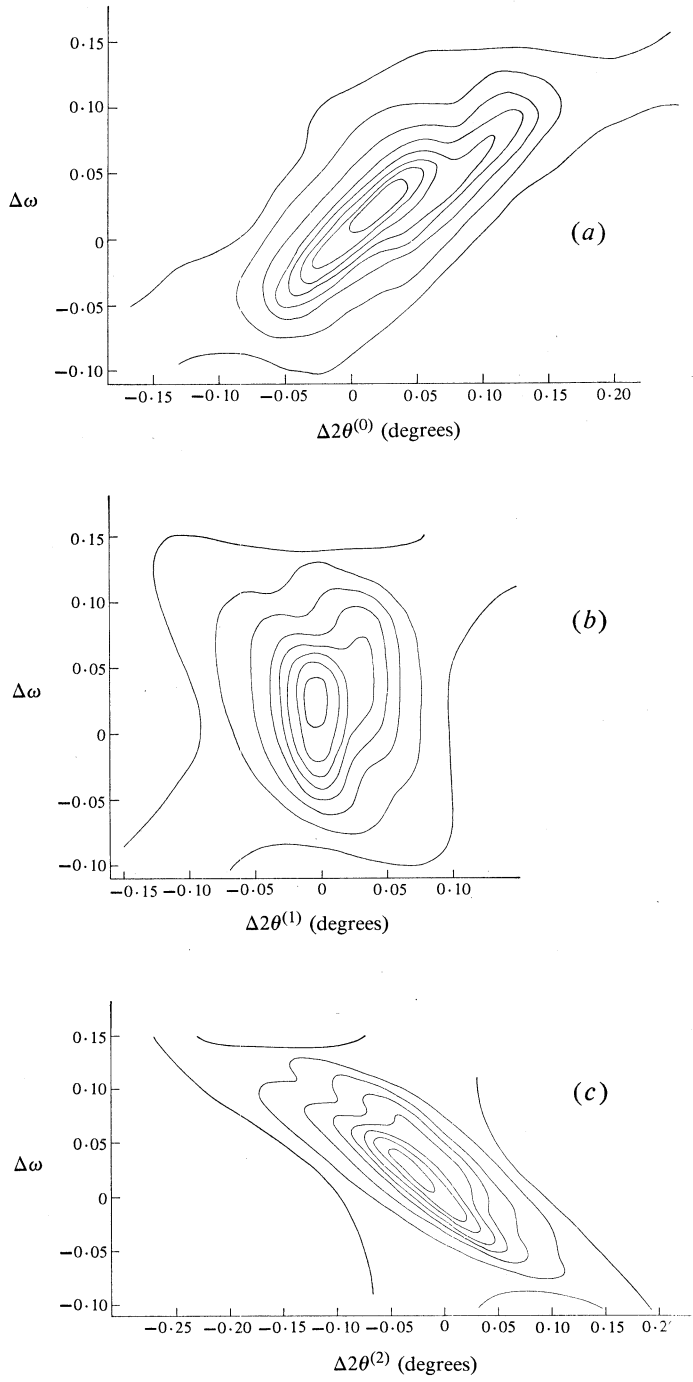

Fig. 2. Measured intensity distribution, $I(\Delta\omega, \Delta 2\theta)$ projected down p, with the set-up in Fig. 1. This distribution is for the $\bar{1}\bar{1}2$ reflection of a small crystal of $CuInSe_2$, using unfiltered Mo Kα radiation. The distribution is presented for (*a*) the ω scan mode, $s = 0$; (*b*) the ω/θ scan mode, $s = 1$; (*c*) the $\omega/2\theta$ scan mode, $s = 2$. The contour levels are 3000, 2500, 2000, 1500, 1000, 500, 200 and 100 counts s^{-1}.

dimension $h \approx 0{\cdot}5$ mm. For completeness, the distribution corresponding to the $\omega/2\theta$ scan mode is shown in Fig. 2*c*.

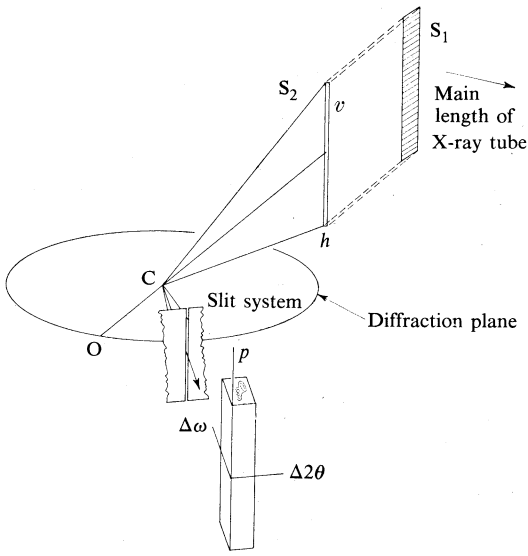

Fig. 3. Experimental arrangement with the main length of the X-ray source S_1 perpendicular to the plane of diffraction, and where S_2, of width h and height v corresponds to the effective source as seen by the specimen crystal C. The aperture system in front of the detector is narrow in the diffraction plane and sufficiently elongated perpendicular to it to collect the total height of the signal. The intensity distribution $I(\Delta\omega, \Delta 2\theta, p)$ of a Bragg reflection, with local reference axes $\Delta\omega$, $\Delta 2\theta$ and p, is indicated in relation to the diffraction plane.

If, instead of the conventional disposition of the source, the X-ray tube is rotated about its main length by 90° so that the main dimension of the source is perpendicular to the diffraction plane and the take-off angle is unchanged at approximately 1 in 10,* then the effective source size, as viewed from the specimen crystal, is greatly reduced in the diffraction plane but presents its full length perpendicular to that plane, say 0·04 by 8 mm for a typical semi-microfocus tube. Fig. 3 illustrates this arrangement showing the resultant three-dimensional distribution $I(\Delta\omega, \Delta 2\theta, p)$. As in Fig. 1, the distribution along p is essentially monotonic but here, because of the extent of v, it will be uniform along most of its length, assuming that the line source emissivity is constant. Since the h dimension is now of the order of 50 μm, the source component σ is very much smaller than in the first case discussed. The v dimension, however, is correspondingly greater so that the X-ray flux incident on the specimen crystal is essentially the same as in the first case. Use of the narrow aperture in front of the detector, but with sufficient vertical extension to receive the signal from the full length of p allows the signal along p to be integrated. One therefore obtains the projected two-dimensional distribution $I(\Delta\omega, \Delta 2\theta)$, the peak intensity being of the same order as in the first case.

* In the present case, the take-off angle was actually 4° or approximately 1 in 14.

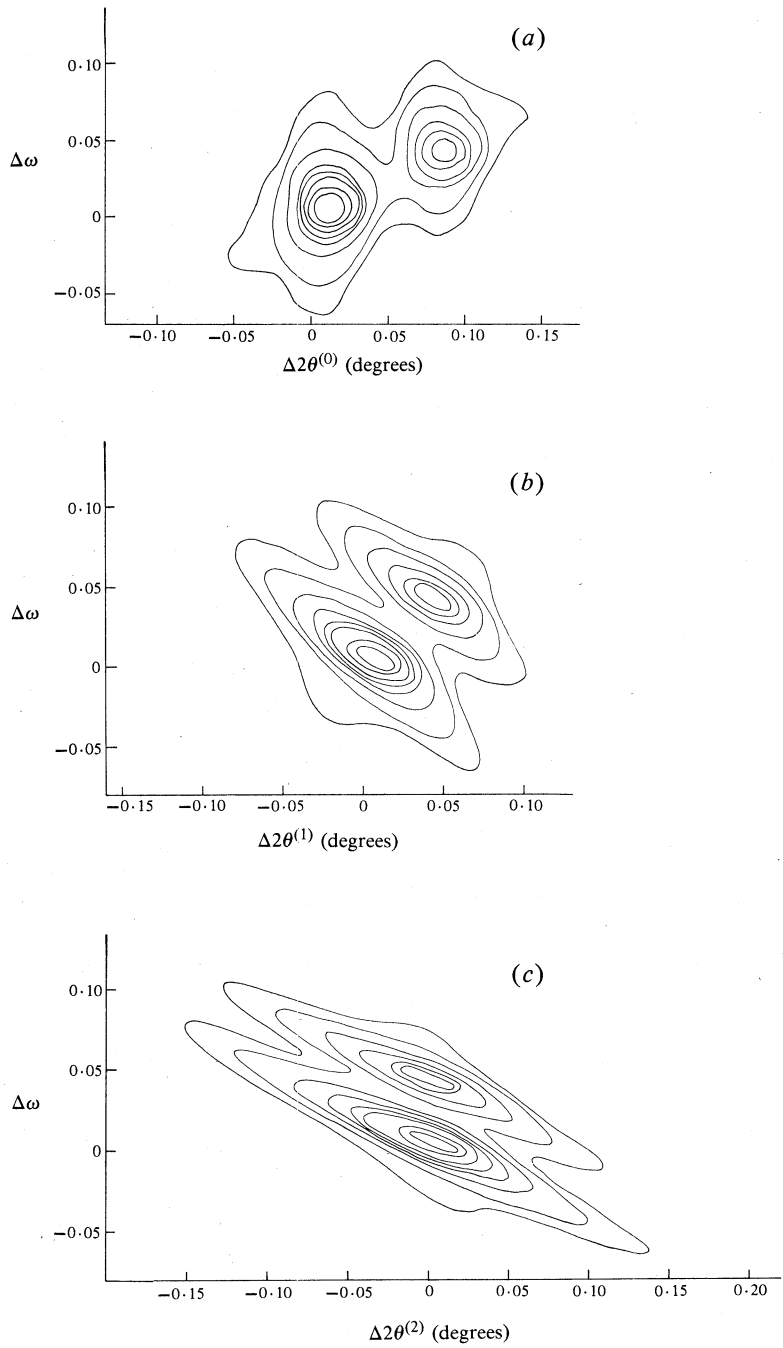

Fig. 4. Measured intensity distribution $I(\Delta\omega, \Delta 2\theta)$ projected down p, with the set-up in Fig. 3. The distribution is for the same reflection and crystal in Fig. 2, namely the $\bar{1}\bar{1}2$ reflection of $CuInSe_2$, using unfiltered Mo Kα radiation. The distribution is given for (*a*) the ω scan mode, $s = 0$; (*b*) the ω/θ scan mode, $s = 1$; (*c*) the $\omega/2\theta$ scan mode, $s = 2$. The contour levels are 4000, 3000, 2000, 1500, 1000, 500, 200 and 100 counts s^{-1}.

The corresponding experimental result for the arrangement in Fig. 3 is shown in Fig. 4*a* for the ω scan mode. For comparison purposes, the distributions corresponding to the ω/θ and $\omega/2\theta$ scan modes are shown in Figs 4*b* and 4*c* respectively.

Comparison of Fig. 4*a* with Fig. 2*a* shows that the σ component is now so small that the existence of the diagnostic slope for that component is not detectable by inspection, even in the ω/θ scan mode (Fig. 4*b*). With this reduction in the component size, the μ and λ components are more clearly resolved [although the dimensional separation of $\lambda(K\alpha_1)$ and $\lambda(K\alpha_2)$ is not, of course, altered]. So, in Fig. 4*a* the distribution parallel to the $\Delta\omega$ axis corresponds essentially to the μ distribution, convoluted by the remaining resolution (or instrument) function, now much reduced by the diminution of the σ component contribution. As noted by Mathieson (1984*b*), the instrumental function could, if required, be established by a test run using a perfect crystal dimensionally equal (or nearly so) to the specimen crystal.

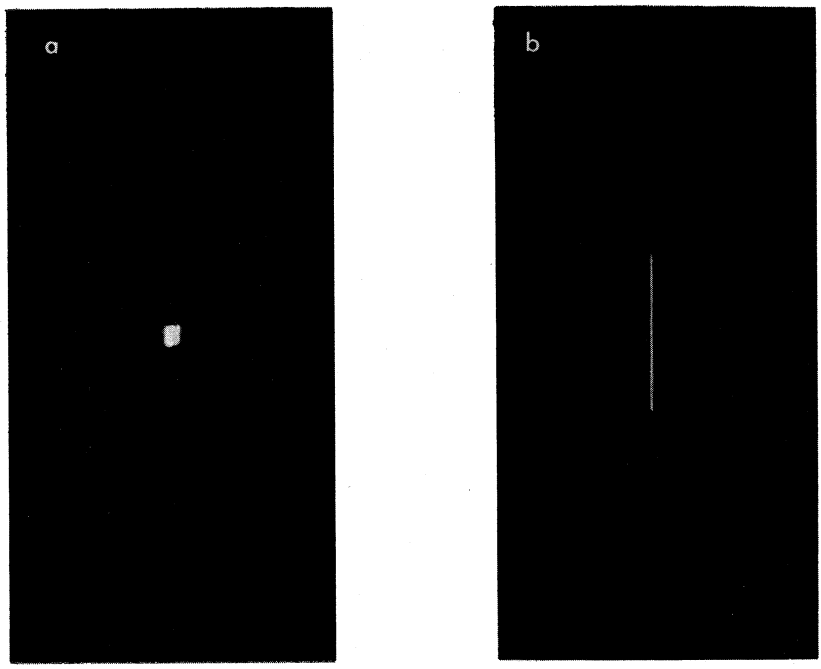

Fig. 5. Photographs of the diffracted beam for the $\bar{1}\bar{1}2$ reflection of $CuInSe_2$ at the detector face (without the aperture) for (*a*) the short source and (*b*) the long source. The diffractometer angles have been optimized for the $K\alpha_1$ wavelength component.

Figs 5*a* and 5*b* are photographs of the diffracted beam for the $\bar{1}\bar{1}2$ reflection of $CuInSe_2$, at the detector face, without the aperture, for the short and long source respectively. The diffractometer angles have been optimized for the $K\alpha_1$ wavelength component. The dimensions of the spot in Fig. 5*a* are approximately $0{\cdot}6\times0{\cdot}5$ mm ($0{\cdot}6\times0{\cdot}4$ mm for the $K\alpha_1$ component alone). Consequently, the introduction of the $\approx0{\cdot}1$ mm wide aperture in front of the detector allows only a fraction of the horizontal signal to pass to the detector. The dimensions of the line in Fig. 5*b* are approximately $4{\cdot}4\times0{\cdot}1$ mm (this being the $K\alpha_1$ component alone). In this case, the $\approx0{\cdot}1$ mm wide aperture passes virtually all of this line.

3. Discussion

In the recent theoretical study of the $\Delta\omega, \Delta 2\theta$ intensity distribution of a Bragg X-ray reflection (Mathieson 1984*b*), attention was drawn to the fact that, by its two-dimensional nature, this new measurement procedure has greater angular resolution and greater information content than the classical one-dimensional reflection profile. Because of these features, the procedure has inherent potential for the more detailed examination of individual reflections, for the intercomparison of different reflections and for improved diagnosis of extinction effects and thus improved accuracy of structure-factor estimation.

To extract exact estimates of the, generally major, individual components μ, σ and λ from such three-component two-dimensional distributions (e.g. Fig. 2) is not, however, a straightforward operation. Initial approximations of the three individual component distributions can be obtained by slice scans (Mathieson 1982) and improved approximations by calculation of $I_{\text{calc}}(\Delta\omega, \Delta 2\theta)$ from these starting points, followed by refinement, matching calculated and measured distributions (say) by difference procedures (Mathieson 1984*b*). While this is a feasible approach, the presence of other, but relatively minor, components in the measured distribution, e.g. that associated with the specimen crystal size and shape (Mathieson 1984*c*), can influence the potential accuracy of the results.

Clearly, reduction from three to two major components would be of considerable advantage in analysing the two-dimensional distribution for the two components which remain, particularly that of the mosaic distribution $\mu(\Delta\omega)$, which is of greatest physical significance because of its relationship to the reflectivity distribution $r(\Delta\omega)$.

The technique outlined here allows for the reduction of the effective size of the source in the diffraction plane, thereby eliminating it as a major component and yet without a consequent loss of peak intensity in the two-dimensional distribution.

The resultant improvement in resolution shown in Fig. 4 relative to that in Fig. 2 is quite striking when one considers that the θ value of the reflection is only $\approx 6{\cdot}1°$. With the improvement in resolution, there is an improvement in the background level relative to that of the peak (improved signal-to-noise ratio). Thus, in Fig. 2, the peak is ≈ 3500 counts s^{-1}, while at the outer edge of the distribution it is ≈ 100 counts s^{-1}; in Fig. 4, the peak has risen to ≈ 4500 counts s^{-1}, while at the outer edge of the distribution it is ≈ 30 counts s^{-1}.

With the reduction in the number of major components to two, those components, whose contributions to the total distribution by comparison are generally small in magnitude, begin to reveal their effects. Observations on these matters and on other results using this measurement procedure will be treated elsewhere.

The present experiment has been carried out on a conventional diffractometer (Picker) and therefore does not represent the highest possible resolution capability of this technique. Nevertheless, it does show that measurement of the $I(\Delta\omega, \Delta 2\theta)$ distribution of a single Bragg reflection by this improved technique can yield an estimate of the reflectivity distribution $r(\Delta\omega)$ (see Mathieson 1984*b*), which is only mildly corrupted by the instrument function. Furthermore, this type of measurement is possible with a relatively simple laboratory set-up and without recourse to highly specialized sources and facilities.

This improved technique using a long source is, of course, applicable to diffraction experiments using radiation other than X rays. In addition, while developed for

small single crystals, it is equally applicable to extended crystals in the Laue mode if a collimator with a small aperture is used just in front of the specimen crystal to explore selected areas.

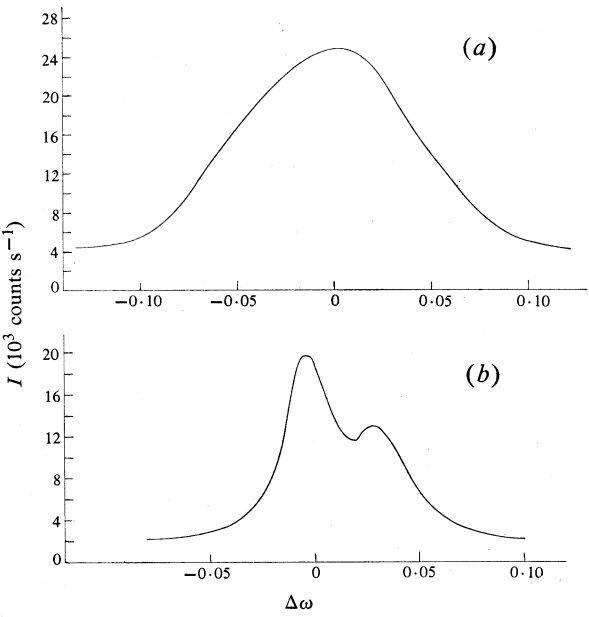

Fig. 6. Results for conventional one-dimensional profile measurements showing the distribution $I(\Delta\omega)$ for (*a*) the short source, by integrating across $\Delta 2\theta$ the data in Fig. 2, and (*b*) the long source, by integrating across $\Delta 2\theta$ the data in Fig. 4.

While this experimental arrangement is particularly advantageous for the new $\Delta\omega, \Delta 2\theta$ procedure, it also offers the possibility of improved results for conventional one-dimensional profile measurements. Fig. 6*a* shows the type of profile curve obtained using a short source; the curve is actually derived by integrating, across $\Delta 2\theta$, the data in Fig. 2. The comparable result in Fig. 6*b* using a long source is derived by a similar operation with Fig. 4. Comparison of these two profiles shows the lower 'background' for the long source data, stressing once more the advantage to be gained, with respect to the signal-to-noise ratio, by the improvement in resolution.

4. Practical Points

The set-up used to obtain the results displayed in Fig. 4 did not use the full length of the X-ray source. The present collimator aperture adjacent to the X-ray tube is that appropriate to an equi-dimensional source (as in Fig. 1), so it only passes a fraction of the full vertical height of the focus available for the new procedure (Fig. 3). With redesign to utilize the full length, greater peak signal would be expected.

The new technique should, of course, be used with appropriate attention to its limitations. The vertical height v used must be such that reflections in the ± 1 cones of reflection for the material under study do not interfere with those in the 0 cone.

To extract the best resolution using the long source, it is advisable to ensure that the line focus of the X-ray source is perpendicular to the diffraction plane and also that it and the narrow aperture are exactly parallel. This can be tested by placing a film in front of the detector with and without the aperture in place.

Acknowledgments

We are deeply grateful to Dr S. L. Mair as the agent of serendipity and to Dr H. J. Whitfield for the crystals of $CuInSe_2$. One of us (A.W.S.) acknowledges the financial support of a CSIRO Postdoctoral Award.

References

Mathieson, A. McL. (1979). *Acta Crystallogr.* A **35**, 50–7.
Mathieson, A. McL. (1982). *Acta Crystallogr.* A **38**, 378–87.
Mathieson, A. McL. (1983). *J. Appl. Crystallogr.* **16**, 257–8.
Mathieson, A. McL. (1984*a*). *Aust. J. Phys.* **37**, 55–61.
Mathieson, A. McL. (1984*b*). *Acta Crystallogr.* A **40**, 355–63.
Mathieson, A. McL. (1984*c*). *J. Appl. Crystallogr.* **17**, 207–9.

Manuscript received 30 May, accepted 9 August 1984